ELSEVIER

Journal of Power Sources 53 (1995) 99–107

JOURNAL OF POWER SOURCES

Gas evolution and performance assessment of submarine lead/acid batteries

J.B. Lakeman [1]

DRA West Drayton, Kingston Lane, West Drayton, Middx. UB7 9QB, UK

Received 22 August 1994; accepted 9 September 1994

Abstract

The gas-evolution rates from new and end-of-life lead/acid submarine cells at both open-circuit and under float-charge have been examined, together with the discharge performance of the cells. The evolved gas is found to comprise hydrogen and oxygen only. The open-circuit and float-charge hydrogen-evolution rates vary logarithmically with temperature. The enthalpy of activation for open-circuit hydrogen evolution is ~70 kJ mol^{-1} for both old and new cells. The open-circuit hydrogen-evolution rate per Ah of rated capacity for new cells is between 0.00636 and 0.105 cm^3 h^{-1} Ah^{-1} at STP at 20–50 °C, respectively. For old cells, a >three-fold increase is observed; the evolution rate ranges from 0.0237 to 0.361 cm^3 h^{-1} Ah^{-1} at STP at 20–50 °C, respectively. On float-charge, using an uncompensated float voltage, the hydrogen-evolution rate of new cells is between 0.0166 and 0.241 cm^3 h^{-1} Ah^{-1} at STP at 20–50 °C, respectively. For old cells, the rates increase to 0.0298–0.903 cm^3 h^{-1} Ah^{-1} at STP at 20–50 °C, respectively. In contrast, the electrical discharge performance of the cells decreases with age. This suggests that the active area for hydrogen evolution increases with age, but that the active area for electrical discharge decreases. No correlation has been established between hydrogen evolution in individual cells and electrical discharge performance for cells of the same age. The self-discharge rates of the negative plates at 20 °C are 14 and 50% per year for new and old cells, respectively.

Keywords: Open-circuit; Float-charge; Gas evolution; Self-discharge; Lead/acid batteries; Submarines

1. Introduction

On-charge gas evolution, and the associated charging efficiency of lead/acid cells, can be used as an indicator of cell condition. The gas evolved derives largely from the electrolysis of water on overcharge, with the components hydrogen and oxygen produced in a fairly constant ratio [1]. Low evolution of gas is associated with better charge retention and lower maintenance (topping up) [2]. On open-circuit, hydrogen evolution is associated with self-discharge of the negative plate, and oxygen with the positive. Therefore, the composition of the evolved gas could vary. On float-charge, it can be assumed that the evolved gas will derive both from self-discharge mechanisms and from the electrolysis of water.

In well-ventilated enclosures, the gassing of aqueous electrolyte batteries does not present a serious hazard. By contrast, in confined spaces, such as in a submarine, gas evolution can pose a serious threat to vehicle safety, and must be kept to a minimum when the vehicle is submerged. It is, therefore, of critical importance that the rate of hydrogen evolution, particularly, is known at all stages of the submarine battery duty cycle, in order that adequate gas-management systems can be designed and implemented.

The increased usage of valve-regulated lead/acid batteries (VRLA) has also highlighted the need to minimize gas evolution, and a great deal of research has already been conducted (see, for example, Refs. [3–6]). The data obtained on very large submarine cells can be extrapolated back to give more accurate information about much smaller systems, for which precise data for gas evolution on open-circuit and float-charge, are not available because of the small amounts of gas evolved.

A report of on-charge gas-evolution experiments on submarine cells has been published previously [1]. The work discussed here concerns the more operationally critical scenario, when the submarine is submerged,

[1] Tel.: 0895 456411.

SSDI 0378-7753(94)02004-M

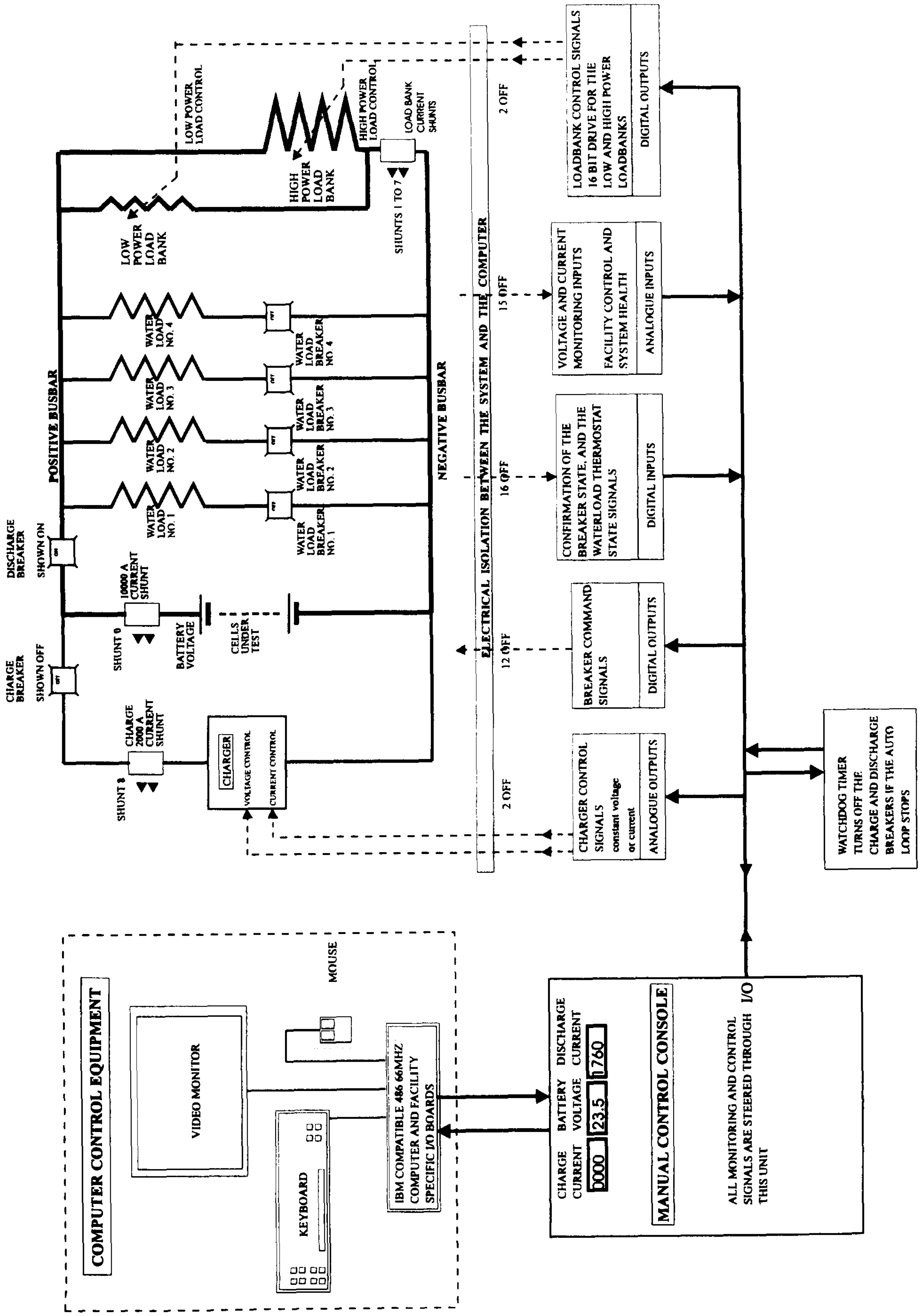

Fig. 1. Schematic diagram of the micro-computer controlled submarine battery test facility at DRA West Drayton.

and the battery is either on open-circuit or on float-charge. The effect of service life on hydrogen-evolution rate is examined by testing both new cells and cells at the end of service. The temperature dependency of gas evolution, and the relationship between evolution rate and electrical discharge performance are also examined.

2. Experimental

Two batteries of submarine cells were tested. In each case the negative grids were made from a binary lead–calcium alloy, and the positive grids were Pb–3wt.%Sb–1.5wt.%Sn–0.05wt.%Se [7]. One battery of ten cells was new and was received in the dry-charged state. The cells were filled with sulfuric acid and cycled to the rated capacity; the rated performance and charging procedure has already been described [1,2]. The second battery, of eight cells, was selected at random from an end-of-life submarine battery.

2.1. Gas evolution

Cells were incubated in a thermostatically-controlled water tank at temperatures ranging from ~11 to 53 °C. Gas-evolution rates were measured either at open-circuit following a full gassing charge, or on a float-charge of 2.20 to 2.22 V/cell. The rate of gas evolution was measured continuously with electronic mass flow-meters. The gas composition was analyzed initially using a quadrupole mass spectrometer, in order to establish that the only significant components were oxygen and hydrogen. Gas compositions were subsequently measured continuously using a paramagnetic oxygen analyzer; the hydrogen content was derived by difference.

2.2. Electrical performance

The discharge performance of the two batteries was measured using a recently developed micro-computer controlled, 16-bit, 0.5 MW battery test facility. A schematic of the facility is shown in Fig. 1. Discharge/charge profiles of up to 45 steps of constant power, current and resistance on discharge, and constant current or voltage on charge, can be programmed in any combination. Discharge is achieved by using resistive loads; the maximum current of 16 000 A is resolved to ~0.25 A. Control precision is limited by the seven current-measuring shunts to better than 0.2% of reading. Charging is carried out using a thyristor-controlled analogue supply.

The discharge current is controlled by arranging the resistive elements into two, 8-bit binary pattern groups: one high power, the other low power. The high-power load bank is shown schematically in Fig. 2. Power MOSFET heat-sink modules are used to switch the individual resistive elements of both banks. For very high power tests, the load is supplemented by four water-cooled resistive loads. A typical five-stage constant power discharge profile on the 10-cell battery is given in Fig. 3.

3. Results and discussion

Fig. 4 illustrates the variation, at open-circuit, of the hydrogen-evolution rate (in $cm^3\ h^{-1}\ cell^{-1}$) at STP

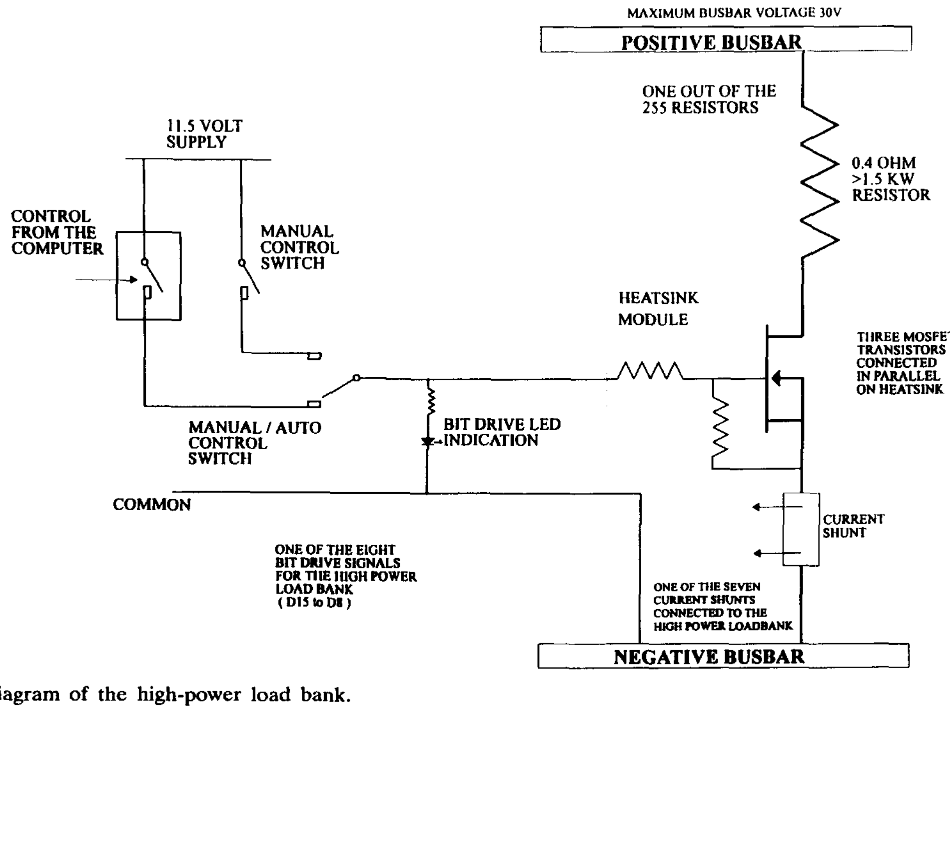

Fig. 2. Schematic diagram of the high-power load bank.

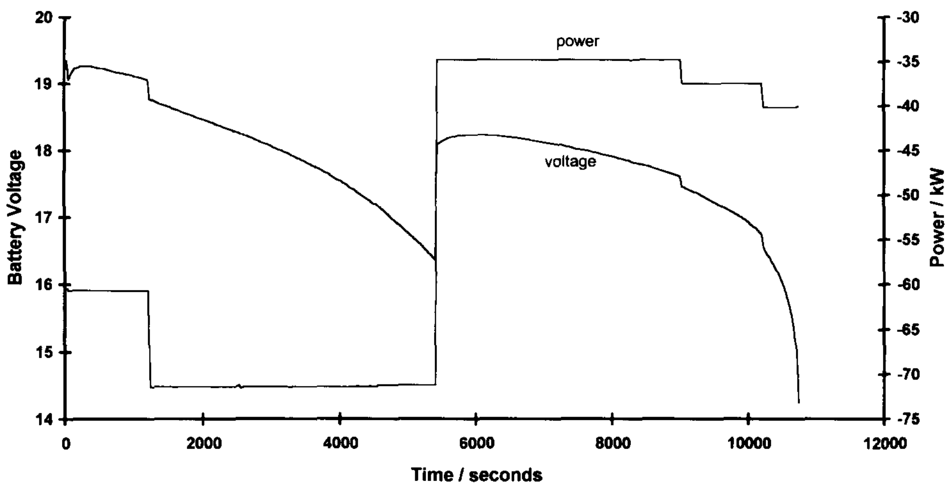

Fig. 3. A five-step constant-power discharge test on 10-cell battery of new cells.

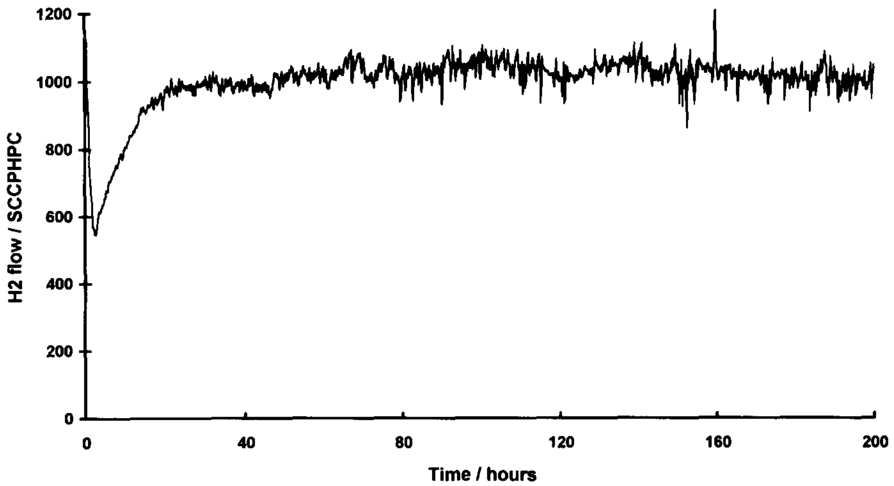

Fig. 4. Average hydrogen-evolution rate vs. time on open-circuit after charge for end-of-life submarine cells at 38 °C.

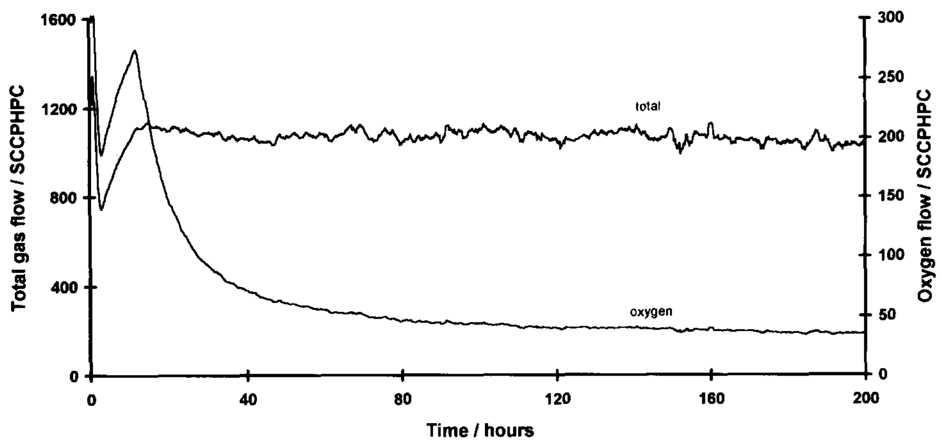

Fig. 5. Average total gas and oxygen-evolution rates vs. time on open-circuit after charge for end-of-life submarine cells at 38 °C.

(SCCPHPC), against time elapsed since a full gassing charge for end-of-life submarine cells at 38 °C. Initially, there is a decrease in flow rate as the residual gas from the previous charge is released. The evolution rate then progressively increases over ~30 h to reach the maximum. The corresponding traces for total gas, and for oxygen, are displayed in Fig. 5. These traces achieve a maximum in ~11 h, following which the oxygen-evolution rate gradually declines. The reason for the decline in oxygen evolution is unclear, but must

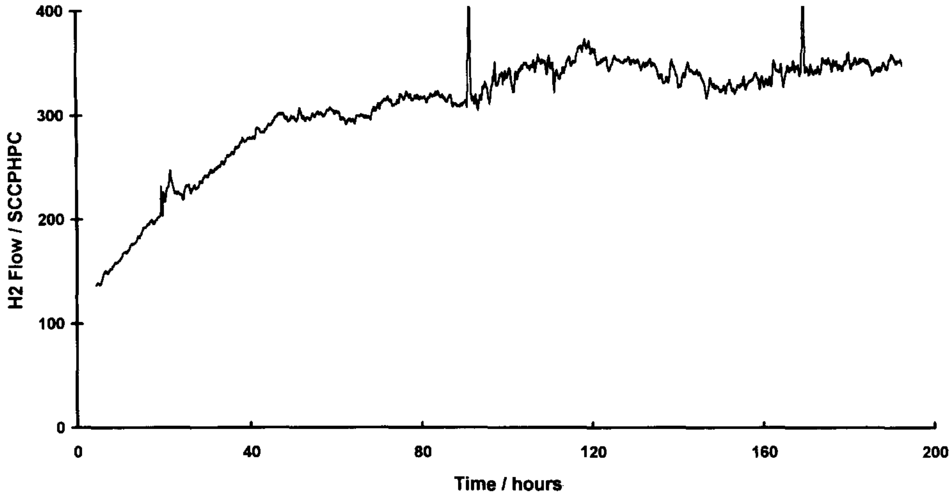

Fig. 6. Average hydrogen-evolution rate vs. time on open-circuit after charge for new submarine cells at 38 °C.

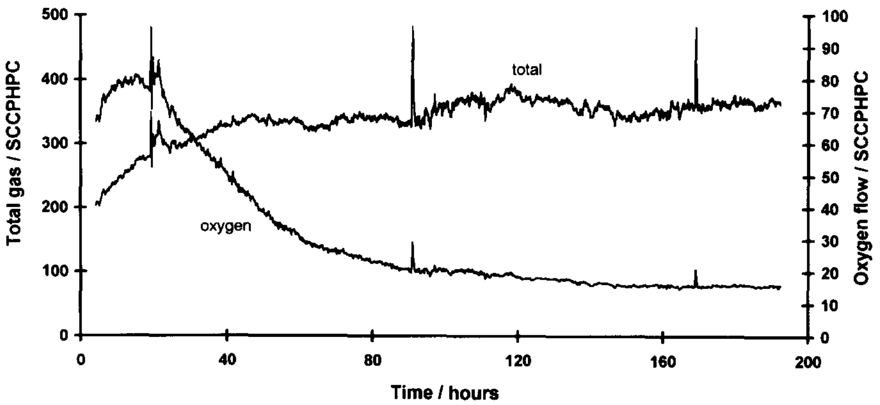

Fig. 7. Average total gas and oxygen-evolution rates vs. time on open-circuit after charge for new submarine cells at 38 °C.

Table 1
Temperature, hydrogen content, and average hydrogen-evolution rate for end-of-life cells on open-circuit

Temperature (°C)	H_2 (%)	H_2 flow rate (SCCPHPC)
11.4	99	89
22	98.5	184
29	98.3	491
29	98.2	536
38	94.5	1307
38	96.7	1026
53	89.8	3707
53.3	90.5	3848

reflect a reduction in the active area for self-discharge at the positive, rather than an increase in the rate of oxygen reduction at the negative.

Fig. 6 illustrates the variation in the average hydrogen-evolution rate at open-circuit with time for new submarine cells at 38 °C. Fig. 7 shows the corresponding traces for total gas and for oxygen. Comparison of Figs. 4 and 5 with Figs. 6 and 7 reveals that the hydrogen-evolution rate rises, and the oxygen-evolution rate falls, more slowly in the case of new cells. The average, steady-state, hydrogen flow-rate for old and new cells at 38 °C was found to be 1040 and 315 SCCPHPC, respectively. This indicates that the open-circuit hydrogen-evolution rate has increased by more than three-fold over the life of the cells.

Results at other temperatures are listed in Tables 1 and 2 for old and new cells, respectively. In each case, the hydrogen content of the evolved gas is always

Table 2
Temperature, hydrogen content, and average hydrogen evolution rate for new cells on open-circuit

Temperature (°C)	H_2 (%)	H_2 flow rate (SCCPHPC)
21	98.9	74
24.3	98.9	94
28.7	98.9	116
34.9	98.9	210
38.3	95.3	361
39.7	98.8	312
44.3	97.2	557
51.5	96.8	1286

90% or above. This confirms previous observations that the rate of self-discharge of the positive is significantly lower than that of the negative [8]. In the case of old cells, there is some indication that the hydrogen content decreases with increasing temperature.

The open-circuit, hydrogen-evolution rate is found to vary logarithmically with temperature, and the results of Tables 1 and 2 are plotted in Figs. 8 and 9, respectively, with the regression equations indicated. From the equations, the open-circuit, hydrogen-evolution rate per Ah of rated capacity for new cells was found to be between 0.00636 and 0.105 $cm^3\ h^{-1}\ Ah^{-1}$ at STP, at 20–50 °C, respectively. For old cells, the corresponding evolution rates are between 0.0237 and 0.361 $cm^3\ h^{-1}\ Ah^{-1}$ at STP.

The slopes of both plots are essentially the same, and the enthalpy of activation for open-circuit hydrogen evolution is calculated as ~70 kJ mol^{-1}. The similarity of slope is illustrated in Fig. 10, but it can be seen that there is an upward shift for the results of end-of-life cells. This suggests that the mechanism for open-circuit hydrogen evolution is the same in both cases, but that the active area for evolution increases with age. This is presumably because of the progressive leaching out of antimony from the positive grid by corrosion, followed by its deposition on the negative active material. Hydrogen is preferentially evolved from local cells on the negative plate between the spongy lead and the deposited antimony [2].

The open-circuit, hydrogen-evolution rates were used to calculate the rate of self-discharge. The data are summarized in Fig. 11. At 20 °C, the self-discharge rates of old and new cells are found to be 50 and 14% per year, respectively; this data should be compared with that of Linden [9]. In the present case, the results show an increased temperature dependency. It should be remembered, however, that the rate is determined by many factors, including the length of storage.

Tables 3 and 4 summarize float-charge data for old and new cells, respectively. The cells were maintained on float-charge, with no temperature compensation of the applied voltage. The float currents achieved for old and new cells are similar, and there is a significant increase in the oxygen content of the evolved gas compared with the open-circuit case. This suggests that there is a Faradaic contribution to gas evolution. The hydrogen content of the evolved gas was greater for the old cells, but did not show any temperature dependence. For the new cells, there is some indication of a decrease in hydrogen content as the temperature increases.

Figs. 12 and 13 again demonstrate a logarithmic relationship of hydrogen-evolution rate with temperature. In this case, the slopes are not the same, and the old cells demonstrate a greater temperature dependence. From the regression equation, the hydrogen evolution rate per Ah of rated capacity for new cells was found to range between 0.0166 and 0.241 $cm^3\ h^{-1}\ Ah^{-1}$ at STP, at 20–50 °C, respectively. For old cells, the corresponding rates were found to lie between 0.0298 and 0.903 $cm^3\ h^{-1}\ Ah^{-1}$ at STP.

The results highlight the significant impact that cell temperature makes on the rate of hydrogen evolution during float charge, when the applied voltage is not

Table 3
Hydrogen-evolution data for end-of-life cells on float-charge

Temperature (°C)	H_2 flow (SCCPHPC)	H_2 (%)	Mean cell voltage (V)	Float current (A)
19.5	198	64	2.208	1.2
23	398	69	2.208	2.3
25	519	69	2.214	2.6
29.5	855	67	2.215	4.3
34	1209	63	2.211	5.5
38	1664	65	2.210	7.2
43	5184	64	2.211	10.0
51.5	7658	71	2.208	16.3

Table 4
Hydrogen-evolution data for new cells on float-charge

Temperature (°C)	H_2 flow (SCCPHPC)	H_2 (%)	Mean cell voltage (V)	Float current (A)
22.4	165	57	2.213	1.9
27	237	54	2.215	2.3
30.7	484	52.5	2.219	4.8
37.8	823	49	2.209	6.7
38	957	50	2.219	7.8
43.2	1332	40	2.218	12.1
48.9	1952	44	2.208	13.3
50.0	1625	47	2.200	15.3

Table 5
Individual hydrogen-evolution rates for old and new cells on float-charge at 38 °C and the individual end-of-discharge voltages (EDV) at the end of *C*/5 rate discharge of the battery

Cell number	Old cells		New cells	
	H_2 flow (SCCPHPC)	EDV (V)	H_2 flow (SCCPHPC)	EDV (V)
1	1731	1.634	915	1.662
2	1604	1.301	960	1.690
3	1659	1.766	964	1.674
4	1680	1.766	981	1.683
5	1664	1.760	944	1.665
6	1678	1.712	974	1.680
7	1831	1.722	965	1.706
8	1463	1.738	955	1.689
Mean	1664	1.675	957	1.681
Standard deviation	104.9	0.157	20.6	0.014

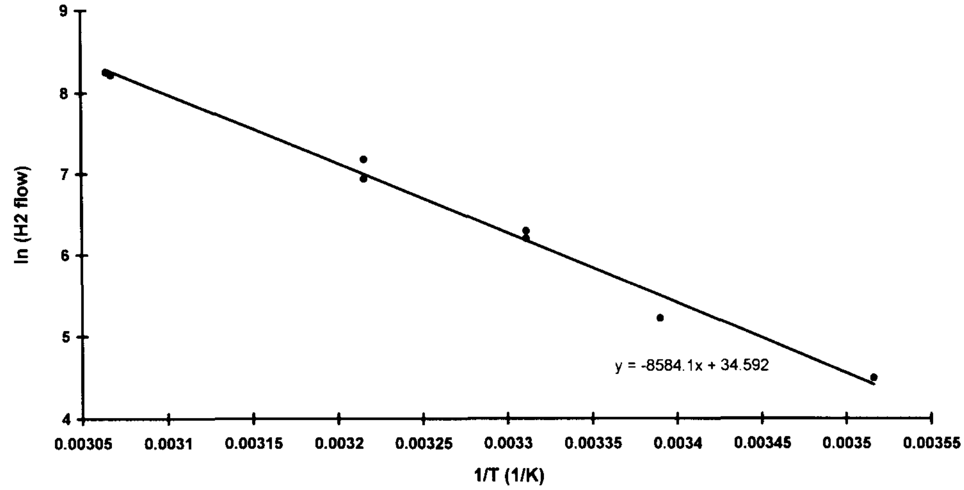

Fig. 8. Plot of ln H_2 flow rate (SCCPHPC) vs. T^{-1} (K^{-1}) for end-of-life cells on open-circuit.

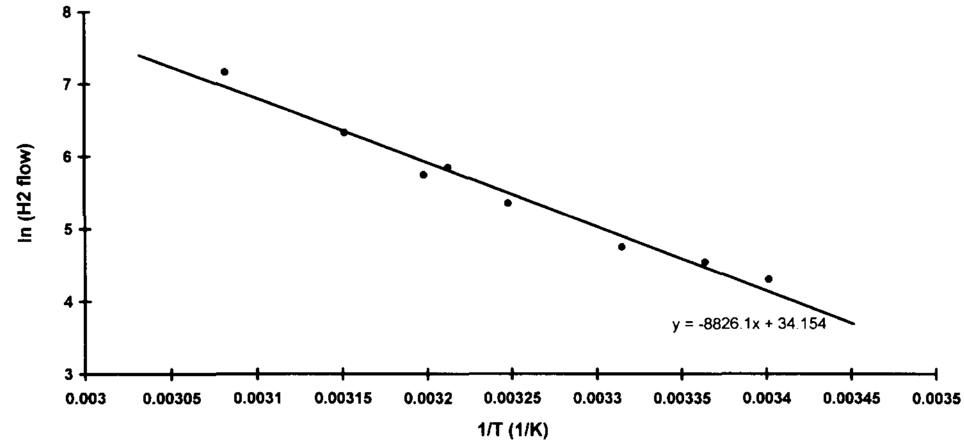

Fig. 9. Plot of ln H_2 flow rate (SCCPHPC) vs. T^{-1} (K^{-1}) new cells on open-circuit.

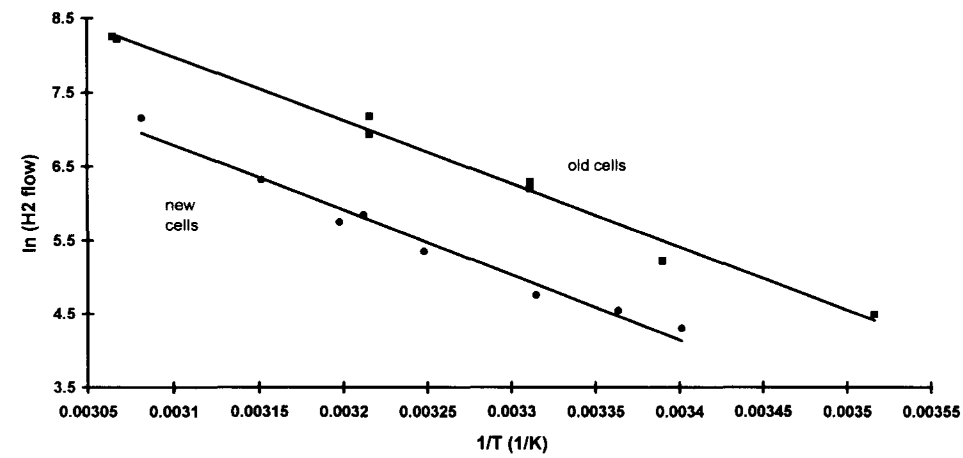

Fig. 10. Plot of ln H_2 flow rate (SCCPHPC) vs. T^{-1} (K^{-1}) for end-of-life and new cells on open-circuit.

compensated for temperature. For new cells, there is a 14-fold increase in rate on moving from 20 to 50 °C; for old cells it is a 30-fold increase. In the confines of a submarine battery tank, individual cell temperatures can vary widely, depending on location. Therefore, large variations in gas-evolution rate can be expected, but effective temperature compensation is not feasible. A similar situation will pertain in any large bank of batteries or cells and adequate precautions must be taken.

The two batteries were discharge tested in order to establish the relationship between the discharge per-

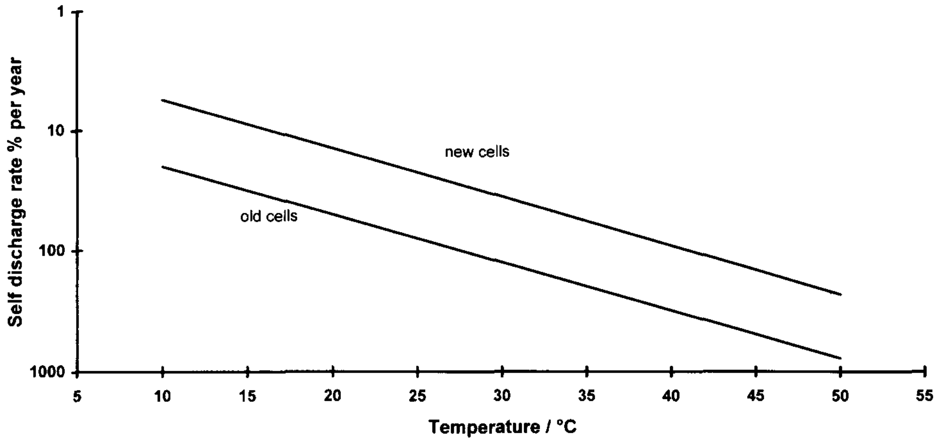

Fig. 11. Plot of rate of self-discharge (% $year^{-1}$) vs. temperature for end-of-life and new submarine cells.

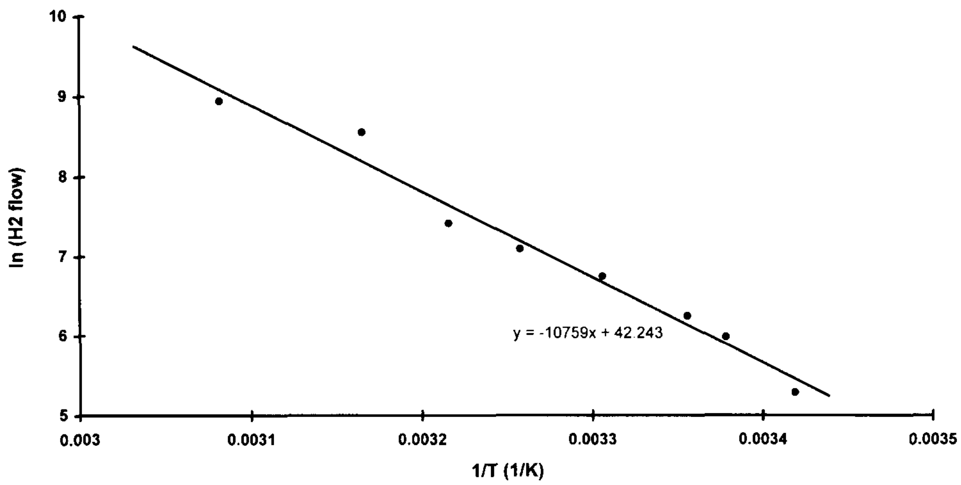

Fig. 12. Plot of ln H_2 flow rate (SCCPHPC) vs. T^{-1} (K^{-1}) for end-of-life cells on float-charge.

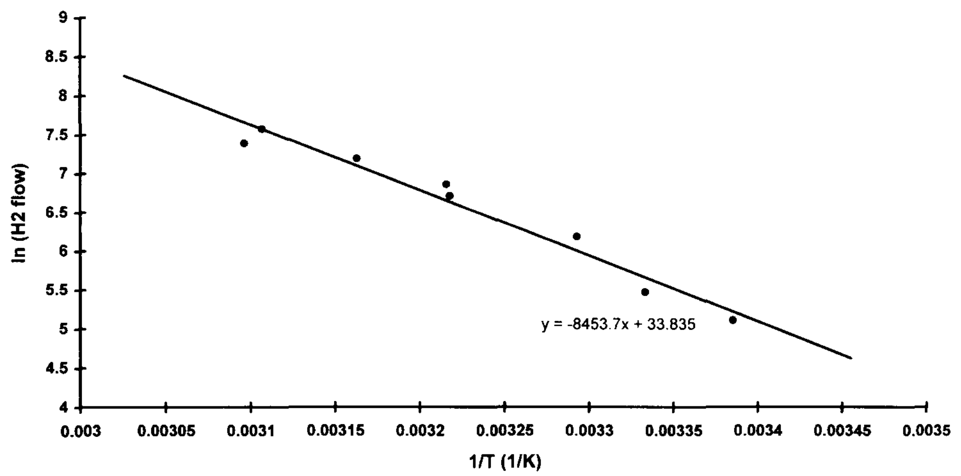

Fig. 13. Plot of ln H_2 flow rate (SCCPHPC) vs. T^{-1} (K^{-1}) for new cells on float-charge.

formance and the hydrogen-evolution rate in cells. At the *C*/5 rate, the end-of-life battery of cells was found to have suffered a 13.7% reduction in capacity over its service life, whilst the battery of new cells achieved the rated capacity. Table 5 lists the individual hydrogen-evolution rates for old and new cells on float-charge at 38 °C. The standard deviations indicate the increased variability in behaviour of old cells compared with new cells. End-of-discharge voltages (EDVs) are also listed for the individual cells at the end of a *C*/5 rate discharge. Again, an increased spread in performance is seen for end-of-life cells. The data also demonstrate that there is no correlation between the discharge performance of individual cells and the corresponding hydrogen-evolution rate. The same behaviour is also observed for cells on open-circuit. The individual cells are consistent, however, in their hydrogen-evolution rates and in their discharge performances. End-of-life cells were found to have suffered a significant reduction in discharge performance over their service life, but the rate of hydrogen evolution on float- or open-circuit significantly increases over the same period. This means that although the active area for electrical discharge has reduced, the active area for hydrogen evolution has increased, probably because of the progressive transference of antimony.

4. Conclusions

1. For cells of the same age, the gas-evolution rate from a cell on open-circuit, or on float-charge, does not correlate with its electrical discharge performance.

2. As a cell ages, its gas-evolution rate increases but its discharge performance decreases. The mechanism for open-circuit hydrogen evolution does not change with age.

3. The active area for hydrogen evolution increases with age, but the active area for discharge decreases.

4. Hydrogen evolution rates at open-circuit and float-charge vary logarithmically with temperature.

5. The open-circuit hydrogen evolution rate can be used as an indicator of the rate of self-discharge of the negative plate.

6. On open-circuit, the rate of self-discharge of the positive plate is significantly lower than that of the negative, and progressively falls with time.

7. Gas-evolution levels when float charging at ~2.2 V/cell are significantly higher than on open-circuit, and the oxygen content is higher.

8. Float charging without compensating the applied voltage for cell temperature can lead to a dramatic increase in the rate of hydrogen evolution as the temperature rises.

References

[1] J.B. Lakeman, *J. Power Sources, 27* (1989) 155–165.
[2] N.E. Bagshaw, *J. Power Sources, 40* (1992) 113–122.
[3] M. Maja and N. Penazzi, *J. Power Sources, 22* 91988) 1–9.
[4] M. Johnson, S.R. Ellis, N.A. Hampson, F. Wilkinson and M.C. Ball, *J. Power Sources, 22* (1988) 11–20.
[5] L.T. Lam, J.D. Douglas, R. Pillig and D.A.J. Rand, *J. Power Sources, 48* (1994) 219–232.
[6] S. Venugopalan, *J. Power Sources, 48* (1994) 371–384.
[7] H. Waterhouse and R. Willows, *Br. Patent No. 622 512* (1949).
[8] A.J. Salkind, G.E. Mayer and D. Linden, in D. Linden (ed.), *Handbook of Batteries and Fuel Cells,* McGraw-Hill, New York, 1984, pp. 14–17.
[9] D. Linden, in D. Linden (ed.), *Handbook of Batteries and Fuel Cells,* McGraw-Hill, New York, 1984, pp. 13–18.